



Integrated gene co-expression network analysis reveals unique developmental processes of *Aurelia aurita*

Wangxiao Xia ^{a,1}, Hui Jiang ^{b,1}, Huifang Guo ^c, Yaowen Liu ^{d,*}, Xingchun Gou ^{a,*}

^a Shaanxi Key Laboratory of Brain Disorders, Institute of Basic Translational Medicine, Xi'an Medical University, Xi'an 710021, China

^b College of Life Science, Hainan Normal University, Haikou 571158, China

^c Shaanxi Key Laboratory of Infection and Immune Disorders, School of Basic Medical Science, Xi'an Medical University, Xi'an 710021, China

^d College of Veterinary Medicine, Yunnan Agricultural University, Kunming 650231, China

ARTICLE INFO

Edited by: Alexander Lewallen

Keywords:

Jellyfish
Development
Gene co-expression network
WGCNA
Module

ABSTRACT

The typical life cycle of the moon jellyfish (*Aurelia aurita*) includes the planula, polyp, strobila, ephyra, and medusa developmental stages. These stages exhibit huge differences in both external morphology and internal physiological functions. However, the gene co-expression network involved in these post-embryonic developmental processes has not been studied yet. Here, based on 15 RNA sequencing samples covering all five stages of the *A. aurita* life cycle, we systematically analyzed the gene co-expression network and obtained 35 relevant modules. Furthermore, we identified the highly correlated modules and hub genes for each stage. These hub genes are implicated to play important roles in the developmental processes of *A. aurita*, which should help improve our understanding of the jellyfish life cycle.

1. Introduction

Jellyfish within the phylum Cnidaria are not only an evolutionarily ancient animal group but also exhibit remarkable and unique post-embryonic development during their life cycle (Gold et al. 2019). Moon jellyfish (*Aurelia aurita*) are characterized by relatively easy breeding and reproduction which are beneficial traits for research. The life cycle of *A. aurita* includes typical five stages i.e. planula polyp strobili ephyra and medusa (Gold et al. 2019). First sperm fertilizes an egg which develops into a free-swimming planula. These motile larvae find suitable sessile substrates on which to attach where they continue to develop into a polyp. The polyp stage consists of a sessile base and tentacles with further develop into a strobila by asexual fission. The strobila separates from the parent body to form an ephyra which eventually develops into a mature medusa with distinct mouth tentacles and reproductive organs (Helm 2018). These stages exhibit substantial differences in both external morphology and internal physiological functions. Thus jellyfish are ideal models to explore the mechanisms underlying post-embryonic developmental processes. To date however

the gene co-expression network involved in the developmental processes of *A. aurita* has not been studied yet.

The advancement of transcriptome-based analyses has provided the opportunity to solve complex questions in the field of developmental biology (Han et al., 2009; González-Porta et al., 2013; Sekhon et al., 2013), including the post-embryonic developmental processes of jellyfish (Fuchs et al., 2014; Brekhman et al., 2015; Khalturin et al., 2019). However, most previous studies have focused on only one or two specific stages or used limited samples to screen differentially expressed genes, without exploring gene co-expression and regulation networks (Fuchs et al., 2014; Brekhman et al., 2015; Khalturin et al., 2019). Weighted gene co-expression network analysis (WGCNA) can be used to explore gene expression connections and networks (Langfelder and Horvath, 2008). Using WGCNA, we can determine the highest correlated gene set (module) for each developmental stage. Furthermore, co-expression network analysis can help identify genes in the center of a network, which are considered to play the most important roles (Liu et al., 2019; Xia et al., 2019; Xia et al., 2019; Li et al., 2020).

In this study, we investigated the transcriptome and gene co-

Abbreviations: WGCNA, Weighted gene co-expression network analysis; RNA-seq, RNA sequencing; PCA, principal component analysis; FPKM, Fragments Per Kilobase of exon model per Million mapped fragments; KEGG, Kyoto Encyclopedia of Genes and Genomes; MEs, module eigengenes; STRING, Search Tool for the Retrieval of Interacting Genes.

* Corresponding authors.

E-mail addresses: yaowenliu@foxmail.com (Y. Liu), gouxingchun@189.cn (X. Gou).

¹ Both these authors contributed equally to this work.

<https://doi.org/10.1016/j.gene.2022.146733>

Received 1 January 2022; Received in revised form 15 June 2022; Accepted 8 July 2022

Available online 18 July 2022

0378-1119/© 2022 Elsevier B.V. All rights reserved.

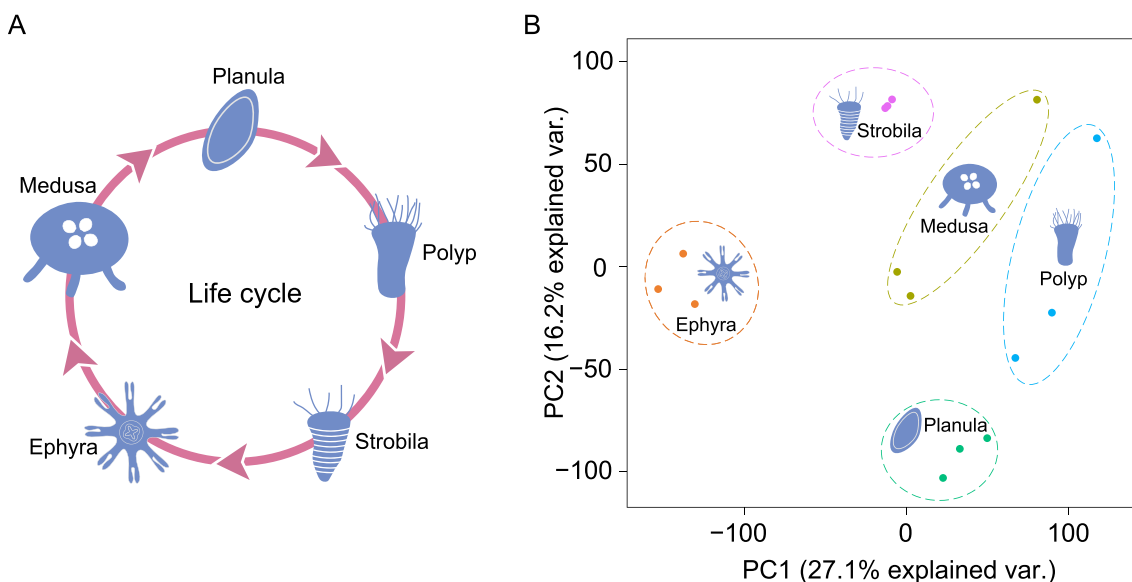


Fig. 1. Principal component analysis of the integrated RNA-seq samples in the life cycle of *A. aurita*. A: The figure shows the typical five developmental stages of the life cycle of *A. aurita*, including planula, polyp, strobila, ephyra and medusa. B: Principal component analysis of the 15 RNA-seq samples.

expression network involved in the post-embryonic developmental processes of *A. aurita*. We successfully identified 35 gene co-expression modules implicated in the developmental processes based on integrated analysis of 15 RNA-seq samples covering all five life cycle stages. Modules highly associated with each developmental stage were identified by correlation analysis, functional annotation, and enrichment analysis. Furthermore, we identified several genes, i.e., *RPS6KA1*, *CTTN*, *CUL1*, *PRPF19*, and *SHH*, in five modules that likely play important roles in the five developmental stages of *A. aurita*. Taken together, these results not only reveal the basis of the gene expression and regulatory network involved in the *A. aurita* life cycle, but also enhance our understanding of the complex cellular and molecular bases underlying the developmental processes of jellyfish.

2. Materials and methods

2.1. Data acquisition

RNA sequencing data were acquired from the NCBI database (accession numbers PRJNA252562, PRJNA490213, PRJNA494057, and PRJNA494062) (Brehman et al., 2015; Gold et al., 2019). In total, 34 RNA-seq samples (planula: five samples; polyp: nine samples; strobila: 10 samples; ephyra: four samples; and medusa: six samples) (Supplementary Table 1) covering the *A. aurita* life cycle were downloaded and integrated from the NCBI database and subjected to transcriptome analysis. Data in SRA format were transformed into *Fastq* format with fastq-dump v2.8.2 (<https://ftp-trace.ncbi.nlm.nih.gov/sra/sdk/2.8.2>).

2.2. Quality control of raw data

Raw sequencing data quality was assessed using FastQC v0.11 (<https://www.bioinformatics.babraham.ac.uk/projects/fastqc/>). Proper thresholds were used to remove low-quality data with Perl scripts (Chen et al., 2019).

2.3. Gene expression profiles

We calculated the gene expression profiles using the filtered high-quality sequencing data with a unifying pipeline. Firstly, the *A. aurita* reference genome was downloaded from the website (<https://davidadlergold.ucdavis.edu/jellyfish/>). The cleaned RNA-seq reads

were mapped to the reference genome using TopHat2 v2.1.1 (Kim et al., 2013). Finally, the mapped reads were assembled into transcripts and gene expression was calculated using Cufflinks v2.2.1 (Trapnell et al., 2010).

2.4. Construction of gene co-expression network by WGCNA

The WGCNA package was installed for co-expression analysis with Bioconductor (<https://bioconductor.org/biocLite.R>) (Langfelder and Horvath, 2008). We calculated the soft thresholding power (β) for network construction using the *pickSoftThreshold* function. The correlation network analyzed with default parameter “unsigned”. Genes with similar expression profiles were identified via the dynamic tree-cutting algorithm with a minimum gene number of 30 in each module and a MEDissThres parameter of 0.25.

2.5. Correlation analysis between developmental stages and modules

The relationships between module eigengenes (MEs) and developmental stages were analyzed to identify significant modules. Using the above acquired gene expression profiles, the modules significantly associated with each developmental stage were analyzed. The correlation index was calculated with the *cor* function and significant differences were determined with the *corPvalueStudent* function.

2.6. Functional and pathway enrichment analyses

To determine the potential functions of the acquired genes, all protein-coding genes in *A. aurita* (<https://davidadlergold.ucdavis.edu/jellyfish/>) were aligned to the Kyoto Encyclopedia of Genes and Genomes (KEGG) database with BLAST v2.6.0 (blastp -query genome.fa -out blast.out -num_alignments 10 -db kegg.database.fa -outfmt 0 -evalue 1e-5). The analysis of biological process enrichment was performed with R (R-3.6.3) depends on Phyper function with parameter lower.tail = FALSE and the p.adjust value was got with parameter BH.

2.7. Construction of protein–protein interaction network

To construct the protein–protein interaction network, we uploaded the protein sequences from one module to the Search Tool for the

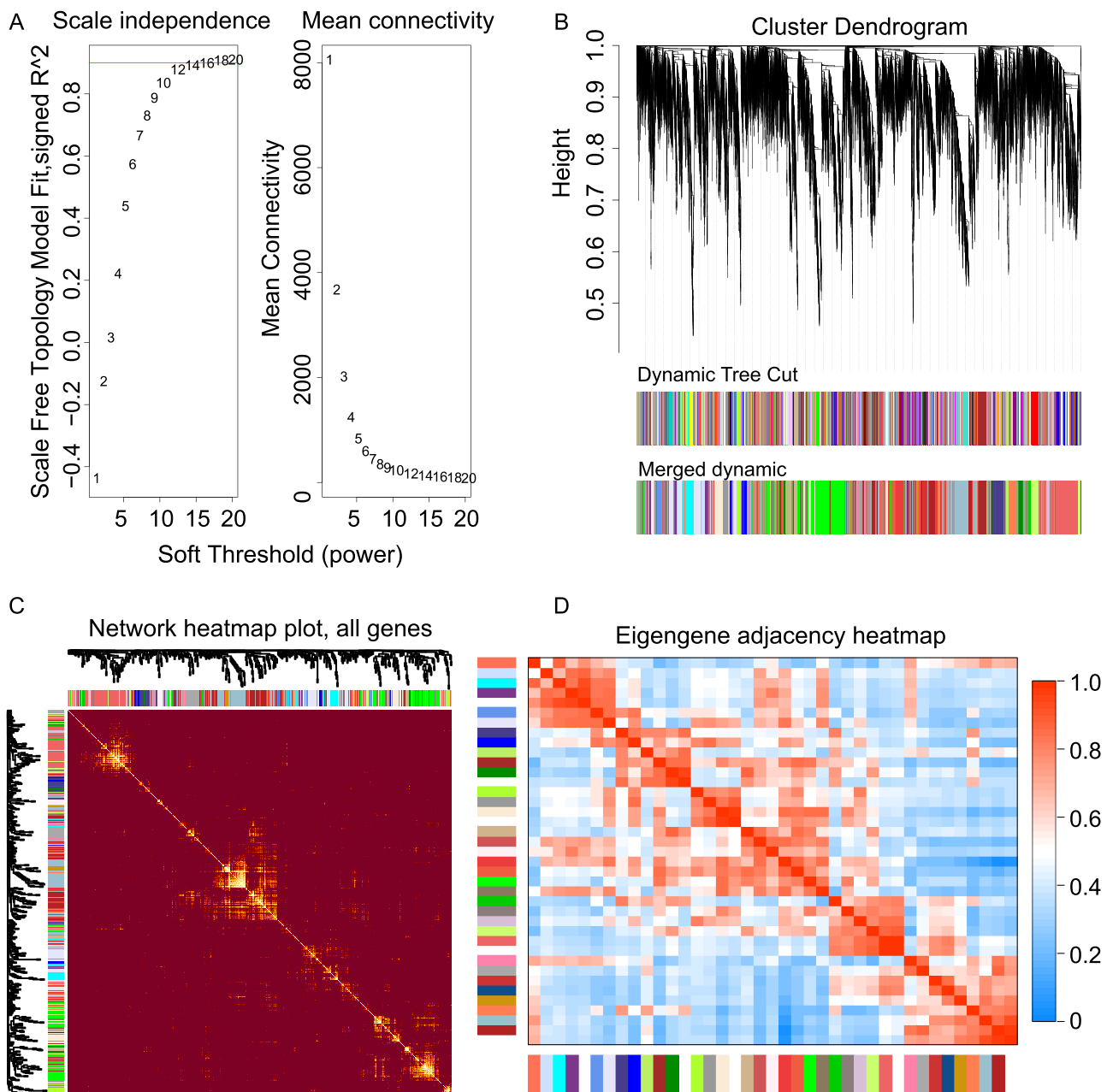


Fig. 2. Co-expression network analysis of genes during the developmental process of *A. aurita*. A: The scale-free fit index of network topology (y-axis) by soft-thresholding power analysis (x-axis). B: Gene dendrogram acquired by hierarchical clustering analysis of adjacency-based dissimilarity. The 35 colors represent 35 modules in the gene co-expression network by WGCNA. C: Heat-map depicts the Topological Overlap Matrix (TOM) among 500 randomly selected genes from the genes hierarchical clustering results. Light yellow color represents higher overlap. D: The heatmap shows the eigengene adjacency. (For interpretation of the references to color in this figure legend, the reader is referred to the web version of this article.)

Retrieval of Interacting Genes (STRING, v10.5) database with a minimum required interaction score of 0.4.

3. Results

3.1. Quality control of integrated large-scale RNA-seq data of *A. aurita*

The life cycle of *A. aurita* includes the planula, polyp, strobila, ephyra, and medusa stages (Fig. 1A). Specifically, 1) planulae develop from fertilized eggs and show swimming capacity through cilia; 2) planulae seek substrates suitable for sessile growth, where they continue to develop into a polyp; 3) polyps consist of a sessile basal plate and upwardly extending tentacles, and develop into strobilae by asexual

fission; 4) subsequently, strobilae separate from the top of the parent body to become ephyrae; 5) ephyrae swim freely in water, maintaining a planktonic form, but eventually develop into mature medusa jellyfish (Fig. 1A). Here, we obtained 34 RNA-seq samples covering all five post-embryonic developmental stages of *A. aurita*. We analyzed the alignment ratio of sequencing reads and principal component analysis (PCA) relationships (Supplementary Fig. 1), with 15 samples finally retained with three biological replicates for each stage (Fig. 1B).

3.2. Construction and analysis of *A. aurita* gene co-expression network

Genes with similar expression patterns may participate in similar biological processes or pathways (Mao et al., 2009). To better

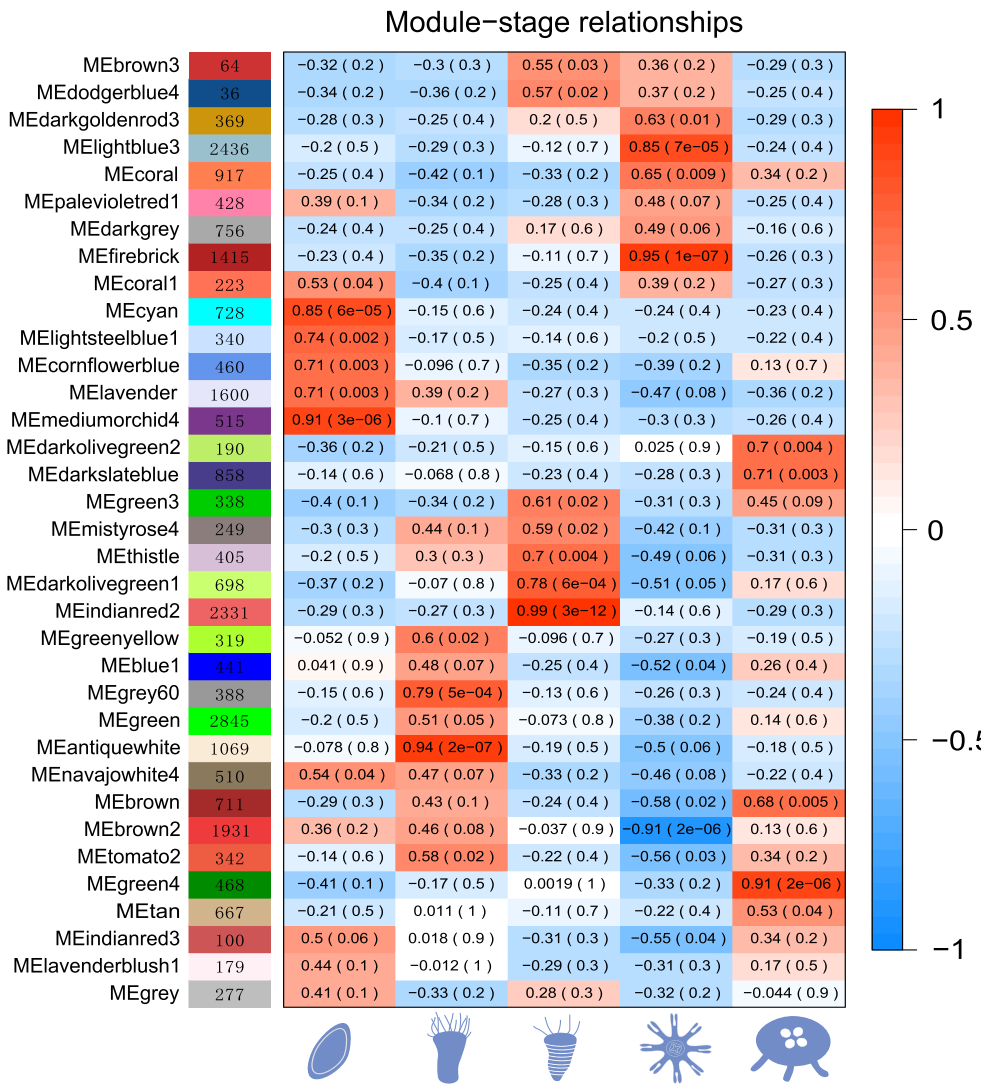


Fig. 3. Module–stage relationships. The numbers shown in each cell represent the p-value and correlation. Each row and column presents a module eigengene and developmental stage in the life cycle, respectively.

understand the biological functions and significance of genes expressed during *A. aurita* development, we analyzed the gene co-expression network by WGCNA to separate genes with similar expression patterns into modules based on average linkage clustering. The soft thresholding power (β) is a critical parameter that can affect average connectivity degree and independence of co-expression modules. We screened network topology using different soft thresholding powers, with $\beta = 18$ (scale free $R^2 = 0.901$) selected for further analysis (Fig. 2A). Furthermore, we performed WGCNA based on hierarchical clustering and constructed the gene co-expression network. We obtained 35 modules after merging modules with a minimum gene number of 30 and using a MEDissThres threshold of 0.25 (Fig. 2B, Supplementary Table 2). In addition, we randomly selected 500 genes from the global weighted co-expression network to construct the topological matrix. Eigengene correlations were used as representative profiles and were applied to quantify module similarity (Fig. 2C). Light-yellow in the topological matrix indicated that the co-expression genes had similar topology.

3.3. Identification of modules highly correlated with each developmental stage in *A. aurita*

To identify modules significantly correlated with the five developmental stages in *A. aurita*, we tested the associations between genes in

each module and developmental stage by WGCNA. Heatmaps showed that many modules were significantly correlated with developmental stages (Fig. 3). For example, the MEmediumorchid4 module was highly correlated with the planula stage ($r = 0.91$, $p = 3 \times 10^{-6}$), MEantiquewhite module with the polyp stage ($r = 0.94$, $p = 2 \times 10^{-7}$), MEindianred2 module with the strobila stage ($r = 0.99$, $p = 3 \times 10^{-12}$), MEfirerbrick module with the ephyra stage ($r = 0.95$, $p = 1 \times 10^{-7}$), and MEmgreen4 module with the medusa stage ($r = 0.91$, $p = 2 \times 10^{-6}$) (Fig. 3).

3.4. Biological functions of highly correlated modules with each developmental stage

To investigate the features of significant modules for each developmental stage, we calculated the average FPKM (Fragments Per Kilobase of exon model per Million mapped fragments) of the three biological replicates for each gene in the respective module and determined the distributions of expression (Fig. 4). Genes in the one highly corrected module of each stage displayed obvious higher distribution pattern of gene expression values in itself than others (Fig. 4). For example, the highly correlated module (MEmediumorchid4) of planula stage showed higher distribution pattern of gene expression values in itself than other module (Fig. 4A).

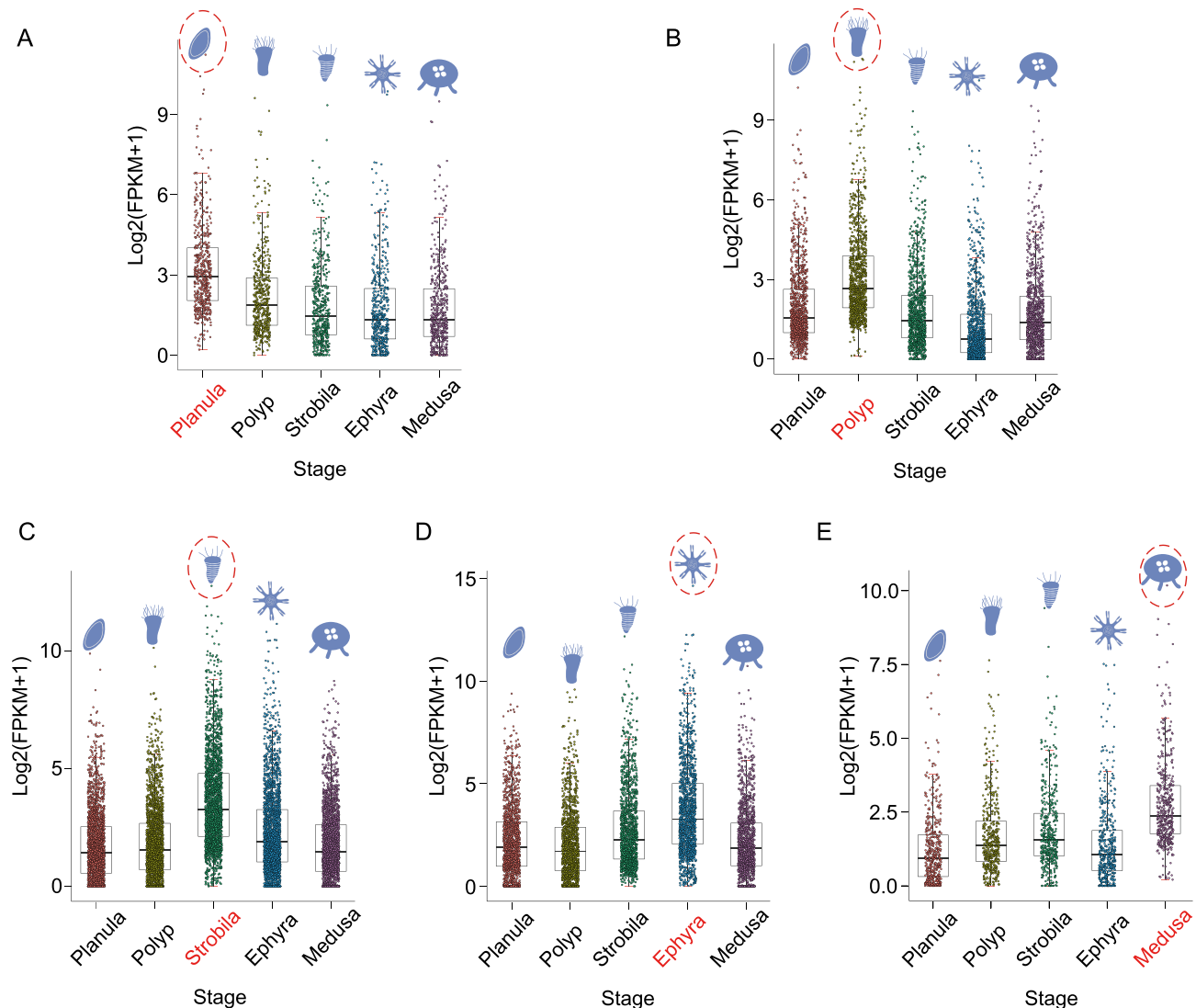


Fig. 4. Expression distributions of genes in the highly-correlated module for each developmental stage. The x-axis shows the developmental stages, and the y-axis shows the transformed value of gene expression value (FPKM). The name of developmental stage we marked red indicates genes in its corresponding highly-correlated module were used for each panel. A: The gene expression profile of MEmediumorchid4 module. B: The gene expression profile of MEantiquewhite module. C: The gene expression profile of MEindianred2 module. D: The gene expression profile of MEfirerbrick module. E: The gene expression profile of MEGreen4 module. (For interpretation of the references to color in this figure legend, the reader is referred to the web version of this article.)

Functions of protein-coding genes were annotated using the KEGG database. Enrichment analysis successfully identified several significant pathways for the five modules (Fig. 5). For the MEmediumorchid4 module, 23 pathways were significantly enriched ($p < 0.05$, Supplementary Table 3), e.g., apoptosis signaling pathway ($p = 4.5 \times 10^{-4}$) (Fig. 5A). For the MEantiquewhite module, 11 pathways were significantly enriched ($p < 0.05$, Supplementary Table 3), e.g., metabolic pathway ($p = 3.0 \times 10^{-4}$) (Fig. 5B). For the MEindianred2 module, 23 pathways were significantly enriched ($p < 0.05$, Supplementary Table 3), e.g., tight junction signaling pathway ($p = 2.9 \times 10^{-3}$) (Fig. 5C). For the MEfirerbrick module, 22 pathways were significantly enriched ($p < 0.05$, Supplementary Table 3), e.g., proteasome signaling pathway ($p = 1.4 \times 10^{-4}$) (Fig. 5D). For the MEGreen4 module, 11 pathways were significantly enriched ($p < 0.05$, Supplementary Table 2), e.g., Hedgehog signaling pathway ($p = 3.0 \times 10^{-4}$) (Fig. 5E). These results suggest that the genes related to these terms likely contribute to the developmental processes of *A. aurita*.

3.5. Interaction network of proteins

First, we analyzed the protein–protein interaction information according to the public database (<https://cn.string-db.org/>). Then, we counted the number of interaction node for each protein. Finally, the core/hub proteins could be identified by ranking the number of interaction node for each protein. One protein with more interaction nodes with other proteins represents it has a more central position in the protein–protein interaction network. In this study, several core genes were found to have more interactions than other genes (Supplementary Table 3). For example, in the MEmediumorchid4 module, the *RPS6KA1* gene (Fig. 6A), which encodes a protein implicated in controlling cell growth and differentiation (Anjum and Blenis, 2008), was located in the center of the protein–protein network. Core genes were also identified in other modules, e.g., the MEantiquewhite module contained *CTTN* (Fig. 6B), which encodes a protein that functions during apoptosis and plays a role in cell migration (Luo et al., 2006); the MEindianred2 module contained *CUL1* (Fig. 6C), which encodes a E3 ubiquitin-protein ligase that mediates the ubiquitination of proteins involved in cell cycle progression, signal transduction, and transcription (Skowyra et al.,

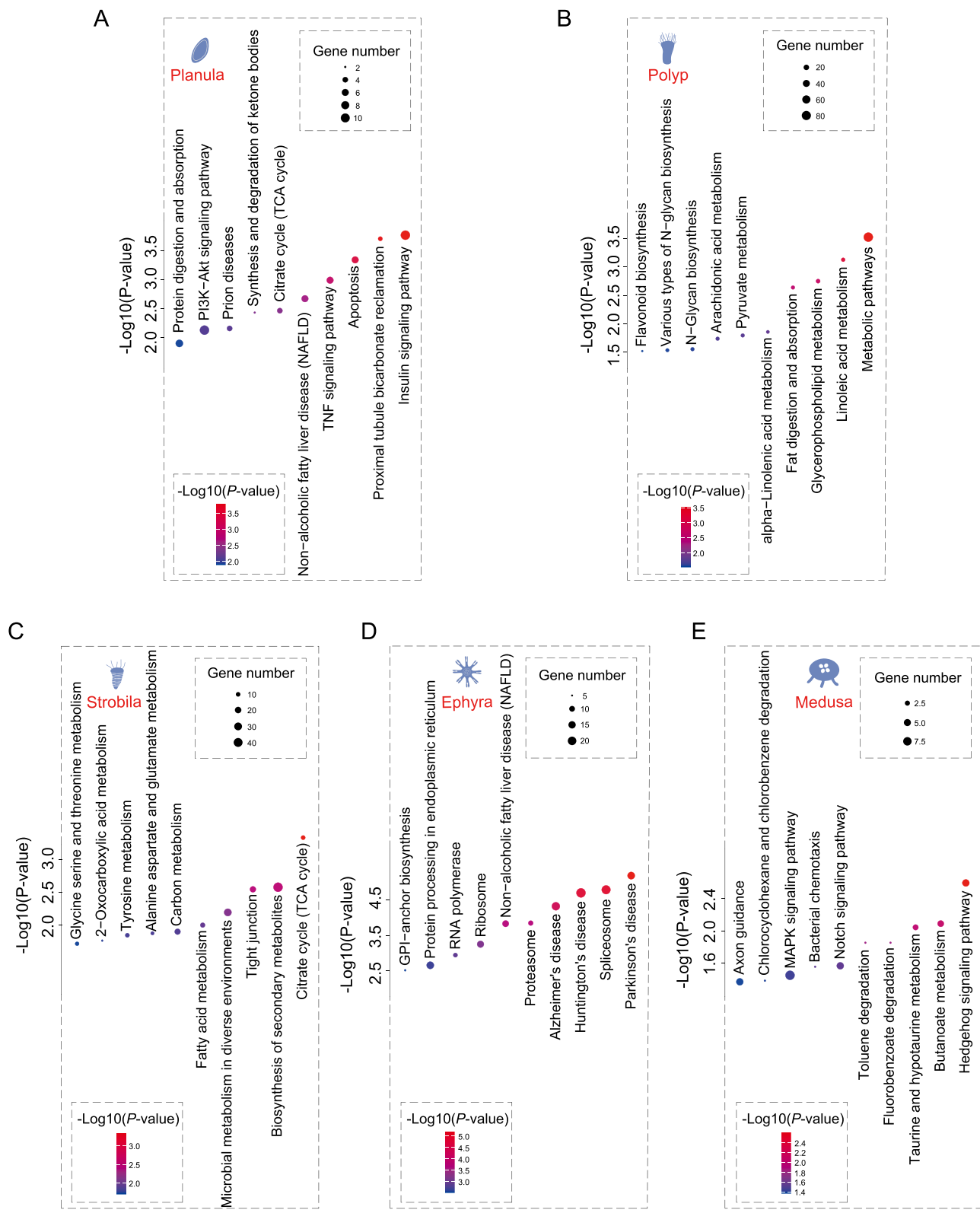


Fig. 5. KEGG enrichment of genes in the five modules. The size and color of the point represents the gene number enriched and the statistical significance (*p*-value) in each pathway, respectively. A: KEGG enrichment of genes in MEmediumorchid4 module.B: KEGG enrichment of genes in MEantiquewhite module. C: KEGG enrichment of genes in MEindianred2 module. D: KEGG enrichment of genes in MEfirerbrick module. D: KEGG enrichment of genes in MEGreen4 module.

1997); the MEfirerbrick module contained *PRPF19* (Fig. 6D), which is essential for cell survival (Chen et al., 2021); and the MEGreen4 module contained *SHH* (Fig. 6E), which encodes a protein instrumental in early embryo patterning (Liu et al., 1998). Taken together, genes described

above located in the central of the protein–protein network have been found play key roles in the developmental and physiological processes and thus may have important functions in the developmental process of the life cycle in *A. aurita*.

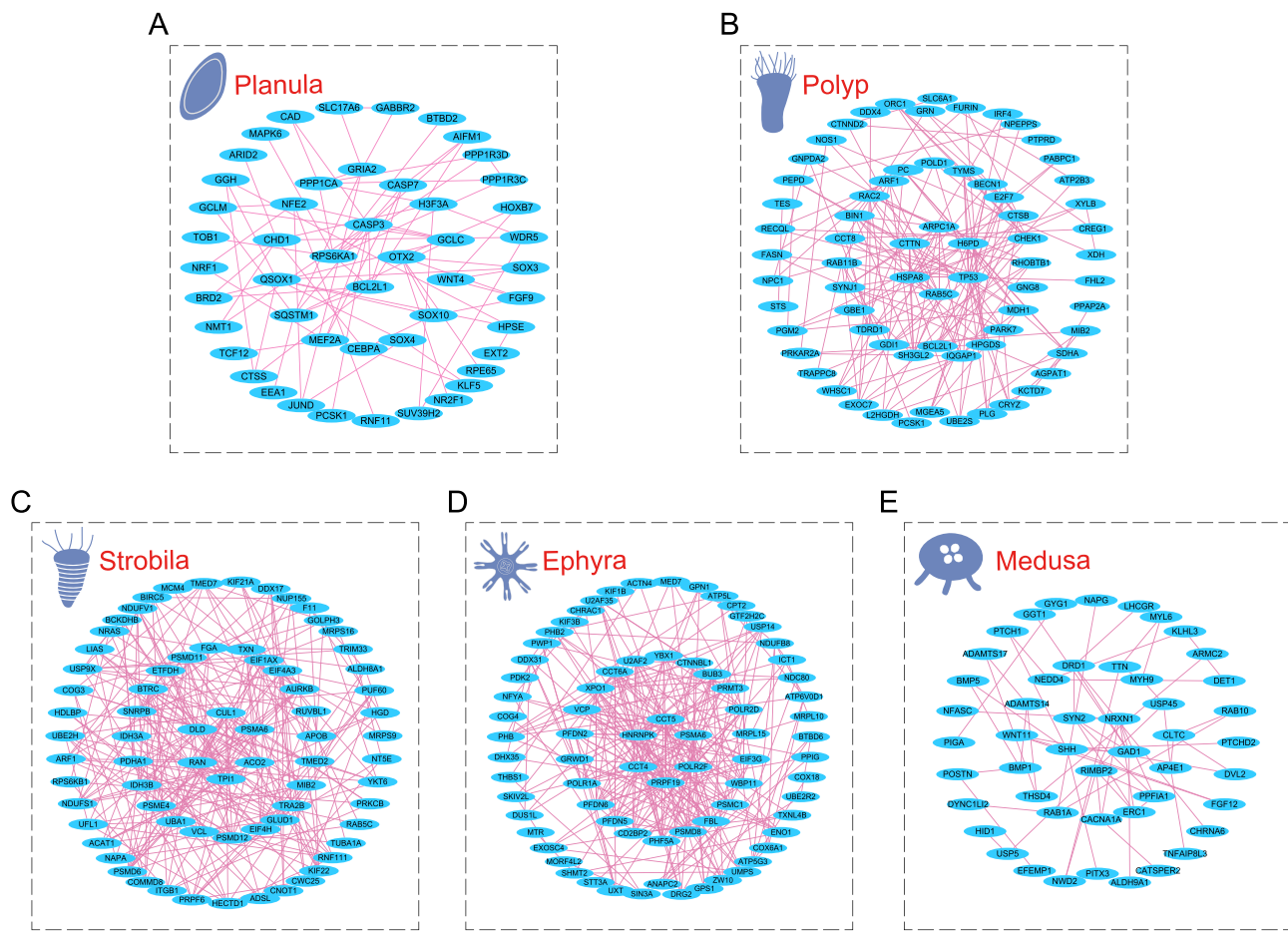


Fig. 6. Networks of protein–protein interactions. The line between two proteins represents the potential interactions. A: Network of protein–protein interactions in MEmediumorchid4 module. B: Network of protein–protein interactions in MEantiquewhite module. C: Network of protein–protein interactions in MEindianred2 module. D: Network of protein–protein interactions in MEfirerbrick module. E: Network of protein–protein interactions in MEGreen4 module.

4. Discussion

Although gene expression during the different life stages of *A. aurita* has been studied for many years, most previous researches have focused on one specific stage or examined limited samples (Fuchs et al., 2014; Brekham et al., 2015; Khalturin et al., 2019). There has been no integrated study of the entire typical life history (planula, polyp, strobila, ephyra, and medusa). In this project, we collected all the published transcriptome data of the five life history stages of jellyfish, 15 samples with the best quality were selected for further study through a series of quality control and screening. Moreover, the gene co-expression network involved in the post-embryonic developmental processes of *A. aurita* has not been elucidated. To clarify the gene regulation network and identify hub genes involved in the developmental processes of the *A. aurita* life cycle at the transcriptomic level, we analyzed the gene co-expression network by WGCNA. We selected a soft thresholding power (β) of 18, which fit index reaches 0.9 of the scale-free topology. Based on this β value, we successfully acquired 35 gene modules, with 277 genes in the gray module not classified, accounting for only 1.08 % of all 25 603 protein-coding genes used. We also performed correlation analysis to identify modules highly correlated with each developmental stage. Results showed that MEmediummorchid4, MEAntiquewhite, MEIndianred2, MEfirerbrick, and MEGreen4 were highly correlated with the planula, polyp, strobila, ephyra, and medusa stages, respectively. Therefore, the genes in these modules may greatly contribute to the developmental processes of the corresponding stages. Genes that have more interactions in the protein–protein network usually perform more critical functions than genes located at the edge. Furthermore, we

analyzed the protein-protein interaction networks using the STRING database with confidence parameter set to more than 0.4 and other parameters were set to default. Based on these results, several genes identified as core genes which have more interactions with other genes, and therefore may play more important roles in the corresponding developmental processes. This study not only revealed the gene co-expression network involved in the developmental processes of the *A. aurita* life cycle, but also furthers our understanding of the complex developmental processes of jellyfish.

5. Conclusions

Based on the integrated analysis of 15 RNA-seq samples covering all five life cycle stages of *A. aurita*, we successfully identified 35 gene co-expression modules during their post-embryonic developmental processes. Modules highly correlated with each stage of the life cycle were identified by the correlation analysis, functional annotation, and enrichment analysis. Furthermore, several genes, i.e., *RPS6KA1*, *CTTN*, *CUL1*, *PRPF19*, and *SHH*, were identified as core genes which have more interactions with other genes, and therefore may play more important roles in the corresponding developmental processes. For example, the gene *SHH*, which was identified as a core gene located in the centre of the protein–protein interaction network in the medusa stage, were implicated as a key inductive signal play roles in multiple developmental processes in previous studies, such as the development of the anterior-posterior limb axis, the ventral neural tube, and the ventral somites (Echeland et al., 1993; Roelink et al., 1994). These results not only reveal the basis of the gene expression and regulatory network during the

development of the life cycle in *A. aurita*, but also enhance our understanding of the complex cellular and molecular bases underlying the developmental processes of jellyfish.

Funding

This research was funded by the National Natural Science Foundation of China (32100406), Chinese Academy of Sciences, State Key Laboratory of Genetic Resources and Evolution, Kunming Institute of Zoology (GREKF21-07), Scientific Research Fund of Shaanxi Provincial Education Department (21JK0888), Natural Science Basic Research Plan in Shaanxi Province of China (2021JQ-775), Research Foundation of Xi'an Medical University (2020DOC26), Natural Science Basic Research Plan in Shaanxi Province of China (2021JM-496).

Author contribution

Wangxiao Xia: Conceptualization, Resources, Data curation, Validation, Writing – original draft. **Hui Jiang:** Resources, Data curation. **Huifang Guo:** Conceptualization. **Yaowen Liu:** Manuscript revision. **Xingchun Gou:** Manuscript revision.

Declaration of Competing Interest

The authors declare that they have no known competing financial interests or personal relationships that could have appeared to influence the work reported in this paper.

Availability of data and materials

All the data used in this study was downloaded from the NCBI database (<https://www.ncbi.nlm.nih.gov/>) and can be accessed with the following accession numbers: PRJNA252562, PRJNA490213, PRJNA494057, and PRJNA494062.

Acknowledgements

We thank Christine Watts for help in honing the manuscript.

Appendix A. Supplementary material

Supplementary data to this article can be found online at <https://doi.org/10.1016/j.gene.2022.146733>.

References

- Anjum, R., Blenis, J., 2008. The RSK family of kinases: emerging roles in cellular signalling. *Nat. Rev. Mol. Cell Biol.* 9 (10), 747–758.
- Brekhman, V., Malik, A., Haas, B., Sher, N., Lotan, T., 2015. Transcriptome profiling of the dynamic life cycle of the scyphozoan jellyfish *aurelia aurita*. *BMC Genomics* 16 (1), 74.
- Chen, Z.S., Huang, X., Talbot, K., Chan, H.Y.E., 2021. A fine balance between Prpf19 and Exoc7 in achieving degradation of aggregated protein and suppression of cell death in spinocerebellar atrophy type 3. *Cell Death Dis.* 12, 136.
- Chen, L., Qiu, Q., Jiang, Y.u., Wang, K., Lin, Z., Li, Z., Bibi, F., Yang, Y., Wang, J., Nie, W., Su, W., Liu, G., Li, Q., Fu, W., Pan, X., Liu, C., Yang, J., Zhang, C., Yin, Y., Wang, Y.u., Zhao, Y., Zhang, C., Wang, Z., Qin, Y., Liu, W., Wang, B., Ren, Y., Zhang, R.u., Zeng, Y., da Fonseca, R.R., Wei, B., Li, R., Wan, W., Zhao, R., Zhu, W., Wang, Y., Duan, S., Gao, Y., Zhang, Y.E., Chen, C., Hvilsom, C., Epps, C.W., Chemnick, L.G., Dong, Y., Mirarab, S., Siegismund, H.R., Ryder, O.A., Gilbert, M.T.P., Lewin, H.A., Zhang, G., Heller, R., Wang, W., 2019. Large-scale ruminant genome sequencing provides insights into their evolution and distinct traits. *Science* 364 (6446). <https://doi.org/10.1126/science:aav6202>.
- Echelard, Y., Epstein, D.J., St-Jacques, B., Shen, L., Mohler, J., McMahon, J.A., et al., 1993. Sonic hedgehog, a member of a family of putative signaling molecules, is implicated in the regulation of CNS polarity. *Cell* 75, 1417–1430.
- Fuchs, B., Wang, W., Graspeuntner, S., Li, Y., Insua, S., Herbst, E.-M., Dirksen, P., Böhm, A.-M., Hemmrich, G., Sommer, F., Domazet-Lošo, T., Klostermeier, U., Anton-Erxleben, F., Rosenstiel, P., Bosch, T.G., Khalturin, K., 2014. Regulation of polyp-to-jellyfish transition in *aurelia aurita*. *Current biology : CB* 24 (3), 263–273.
- Gold, D.A., Katsuki, T., Li, Y., Yan, X., Regulski, M., Iberson, D., Holstein, T., Steele, R. E., Jacobs, D.K., Greenspan, R.J., 2019. The genome of the jellyfish *aurelia* and the evolution of animal complexity. *Nat. Ecol. Evol.* 3 (1), 96–104.
- González-Porta, M., Frankish, A., Rung, J., Harrow, J., Brazma, A., 2013. Transcriptome analysis of human tissues and cell lines reveals one dominant transcript per gene. *Genome Biol.* 14 (7), R70. <https://doi.org/10.1186/gb-2013-14-7-r70>.
- Han, X., Wu, X., Chung, W.-Y., Li, T., Nekrutenko, A., Altman, N.S., Chen, G., Ma, H., 2009. Transcriptome of embryonic and neonatal mouse cortex by high-throughput rna sequencing. *PNAS* 106 (31), 12741–12746.
- Helm, R.R., 2018. Evolution and development of scyphozoan jellyfish. *Biol. Rev. Camb. Philos. Soc.* 93 (2), 1228–1250.
- Khalturin, K., Shinzato, C., Khalturina, M., Hamada, M., Fujie, M., Koyanagi, R., Kanda, M., Goto, H., Anton-Erxleben, F., Toyokawa, M., Toshino, S., Satoh, N., 2019. Medusozoan genomes inform the evolution of the jellyfish body plan. *Nat. Ecol. Evol.* 3 (5), 811–822.
- Kim, D., Pertea, G., Trapnell, C., Pimentel, H., Kelley, R., Salzberg, S.L., 2013. Tophat2: Accurate alignment of transcriptomes in the presence of insertions, deletions and gene fusions. *Genome Biol.* 14 (4), R36. <https://doi.org/10.1186/gb-2013-14-4-r36>.
- Langfelder, P., Horvath, S., 2008. Wgcna: An r package for weighted correlation network analysis. *BMC Bioinf.* 9, 559.
- Li, W., Wang, L., Wu, Y., Yuan, Z., Zhou, J., 2020. Weighted gene co-expression network analysis to identify key modules and hub genes associated with atrial fibrillation. *Int. J. Mol. Med.* 45 (2), 401–416.
- Liu, Y., Gu, H.Y., Zhu, J., Niu, Y.M., Zhang, C., Guo, G.L., 2019. Identification of hub genes and key pathways associated with bipolar disorder based on weighted gene co-expression network analysis. *Front. Physiol.* 10, 1081.
- Liu, A., Joyner, A.L., Turnbull, D.H., 1998. Alteration of limb and brain patterning in early mouse embryos by ultrasound-guided injection of Shh-expressing cells. *Mech. Dev.* 75 (1-2), 107–115.
- Luo, M.L., Shen, X.M., Zhang, Y., Wei, F., Xu, X., Cai, Y., et al., 2006. Amplification and overexpression of ctnn (ems1) contribute to the metastasis of esophageal squamous cell carcinoma by promoting cell migration and anoikis resistance. *Cancer Research* 66 (24), 11690.
- Mao, L., Van Hemert, J.L., Dash, S., Dickerson, J.A., 2009. Arabidopsis gene co-expression network and its functional modules. *BMC Bioinf.* 10, 346.
- Roelink, H., Augsburger, A., Heemskerk, J., Korzh, V., Norlin, S., Ruiz i Altaba, A., et al., 1994. Floor plate and motor neuron induction by vhh-1, a vertebrate homolog of hedgehog expressed by the notochord. *Cell* 76: 761-775.
- Sekhon, R.S., Briskine, R., Hirsch, C.N., Myers, C.L., Springer, N.M., Buell, C.R., et al., 2013. Maize gene atlas developed by rna sequencing and comparative evaluation of transcriptomes based on rna sequencing and microarrays. *PLoS one* 8 (4), e61005.
- Skowyra, D., Craig, K.L., Tyers, M., Elledge, S.J., Harper, J.W., 1997. F-box proteins are receptors that recruit phosphorylated substrates to the SCF ubiquitin-ligase complex. *Cell* 91 (2), 209–219.
- Trapnell, C., Williams, B.A., Pertea, G., Mortazavi, A., Kwan, G., van Baren, M.J., Salzberg, S.L., Wold, B.J., Pachter, L., 2010. Transcript assembly and quantification by rna-seq reveals unannotated transcripts and isoform switching during cell differentiation. *Nat. Biotechnol.* 28 (5), 511–515.
- Xia, W.X., Yu, Q., Li, G.H., Liu, Y.W., Xiao, F.H., Yang, L.Q., et al., 2019a. Identification of four hub genes associated with adrenocortical carcinoma progression by wgcna. *PeerJ* 7, e6555.
- Xia, W.-X., Zhang, L.-H., Liu, Y.-W., 2019b. Weighted gene co-expression network analysis reveals six hub genes involved in and tight junction function in pancreatic adenocarcinoma and their potential use in prognosis. *Genet. Test. Mol. Biomarkers* 23 (12), 829–836.